Organometallics **2002,** *21,* 4065−4075

Activations of Silanes with $[PhB(CH_2PPh_2)_3]Ir(H)(\eta^3\text{-}C_8H_{13})$. Formation of Iridium Silylene Complexes via the Extrusion of Silylenes from Secondary Silanes R_2SiH_2

Jay D. Feldman, Jonas C. Peters,[†] and T. Don Tilley*

Department of Chemistry, University of California at Berkeley,
Berkeley, California 94720-1460

Received May 13, 2002

The abstraction of methide from $(Me_3P)_3Ir(SiHMes_2)(Me)(H)$ (**1**) with $B(C_6F_5)_3$ gave the silylene complex $[fac\text{-}(Me_3P)_3(H)_2Ir(SiMes_2)][MeB(C_6F_5)_3]$ (**2**) via 1,2-hydrogen migration. Secondary silanes (H_2SiR_2) reacted with $[PhBP_3]Ir(H)(\eta^3\text{-}C_8H_{13})$ (**3**) (where $[PhBP_3] = PhB(CH_2PPh_2)_3^-$) to give silylene complexes of the type $[PhBP_3](H)_2Ir{=}SiR_2$ (R = 2,4,6-trimethylphenyl (Mes), **4a**; R = Ph, **4b**; R = Et, **4c**; R = Me, **4d**), with loss of cyclooctene. Analogously, the germylene complex $[PhBP_3](H)_2Ir{=}GeMes_2$ was obtained via the reaction of **3** with Mes_2GeH_2. Primary silanes (H_3SiR) reacted with **3** to give $[PhBP_3](H)_2Ir{=}Si(R)(c\text{-}C_8H_{15})$ (R = Mes, **8a**; R = 2,4,6-triisopropylphenyl (Trip), **8b**) via an intermediate silylene complex with an Si−H bond, $[PhBP_3](H)_2Ir{=}Si(R)(H)$. With tertiary silanes (R_3SiH), silyl-capped trihydride complexes of the type $[PhBP_3]IrH_3(SiR_3)$ (R = Et, **7a**; R = Me, **7b**) and 1,3-cyclooctadiene were produced. The mechanisms of these processes are discussed.

Introduction

Transition-metal silylene chemistry has evolved significantly since the first silylene complexes were reported in 1990.[1] This class of compounds is important to the development of organosilicon chemistry, as numerous reactions of organosilanes are thought to occur via intermediate silylene complexes.[2−7] Furthermore, since carbene complexes are useful in organic synthesis, it is possible that analogous silylene complexes may be valuable as catalysts and synthetic intermediates in organosilicon chemistry.

Synthetic approaches to silylene complexes include triflate[1,8−11] or chloride[12] abstraction from silicon to yield cationic complexes of the type $L_nM{=}SiR_2^+$ (eq 1), the coordination of free silylenes (as stable diamide compounds[13−17] or as generated photochemically[18]) to transition metals (eq 2), and the induced migration of H from Si to Pt upon abstraction of Me^- from (dippe)Pt(Me)(SiHMes$_2$) (eq 3; dippe = $^iPr_2PCH_2CH_2P^iPr_2$, Mes = 2,4,6-trimethylphenyl).[19] The last process, based on 1,2-migration, is of interest because silylene-containing intermediates produced in this way have often been proposed to account for rearrangements in metal silyl complexes.[2−7,20−30] In addition, the participation of silylene complexes in catalytic cycles would seem to require a two-step activation of the silane substrate, involving initial oxidative addition of the silane followed by a 1,2-migration to produce the silylene ligand (eq 4).

[†] Current address: Division of Chemistry and Chemical Engineering, California Institute of Technology, Pasadena, CA 91125.

(1) Straus, D. A.; Grumbine, S. D.; Tilley, T. D. *J. Am. Chem. Soc.* **1990**, *112*, 7801.

(2) Tilley, T. D. In *The Silicon-Heteroatom Bond*; Patai, S., Rappoport, Z., Eds.; Wiley: New York, 1991; pp 245, 309.

(3) Tilley, T. D. In *The Chemistry of Organic Silicon Compounds*; Patai, S., Rappoport, Z., Eds.; Wiley: New York, 1989; p 1415.

(4) Tilley, T. D. *Comments Inorg. Chem.* **1990**, *10*, 37.

(5) Corey, J. In *Advances in Silicon Chemistry*; JAI Press: Greenwich, CT, 1991; Vol. 1, p 327.

(6) Pannell, K. H.; Sharma, H. *Chem. Rev.* **1995**, *95*, 1351.

(7) Zybill, C. *Top. Curr. Chem.* **1991**, *160*, 1.

(8) Grumbine, S. D.; Tilley, T. D.; Arnold, F. P.; Rheingold, A. L. *J. Am. Chem. Soc.* **1993**, *115*, 7884.

(9) Grumbine, S. D.; Tilley, T. D.; Rheingold, A. L. *J. Am. Chem. Soc.* **1993**, *115*, 358.

(10) Grumbine, S. K.; Tilley, T. D.; Arnold, F. P.; Rheingold, A. L. *J. Am. Chem. Soc.* **1994**, *116*, 5495.

(11) Grumbine, S. K.; Mitchell, G. P.; Straus, D. A.; Tilley, T. D.; Rheingold, A. L. *Organometallics* **1998**, *17*, 5607.

(12) Wanandi, P. W.; Glaser, P. B.; Tilley, T. D. *J. Am. Chem. Soc.* **2000**, *122*, 972.

(13) Denk, M.; Hayashi, R. K.; West, R. *Chem. Commun.* **1994**, 33.

(14) Gehrhus, B.; Hitchcock, P. B.; Lappert, M. F.; Maciejewski, H. *Organometallics* **1998**, *17*, 5599.

(15) Petri, S. H. A.; Eikenberg, D.; Neumann, B.; Stammler, H.-G.; Jutzi, P. *Organometallics* **1999**, *18*, 2615.

(16) Cai, X. P.; Gehrhus, B.; Hitchcock, P. B.; Lappert, M. F.; Maciejewski, H. *Can. J. Chem.* **2000**, *78*, 1484.

(17) Amoroso, D.; Haaf, M.; Yap, G. P. A.; West, R.; Fogg, D. E. *Organometallics* **2000**, *21*, 534.

(18) Feldman, J. D.; Mitchell, G. P.; Nölte, J.-O.; Tilley, T. D. *J. Am. Chem. Soc.* **1998**, *120*, 11184.

(19) Mitchell, G. P.; Tilley, T. D. *Angew. Chem., Int. Ed.* **1998**, *37*, 2524.

(20) Sharma, H. K.; Pannell, K. H. *Chem. Rev.* **1995**, *95*, 1351.

(21) Sharma, S.; Pannell, K. H. *Organometallics* **2001**, *20*, 7.

(22) Pannell, K. H.; Sharma, H. K.; Kapoor, R. N.; Cervantes-Lee, F. *J. Am. Chem. Soc.* **1997**, *119*, 9315.

(23) Pannell, K. H.; Brun, M. C.; Sharma, H.; Jones, K.; Sharma, S. *Organometallics* **1994**, *13*, 1075.

(24) Okazaki, M.; Tobita, H.; Kawano, Y.; Inomata, S.; Ogino, H. *J. Organomet. Chem.* **1998**, *553*, 1.

(25) Ueno, K.; Asami, S.; Watanabe, N.; Ogino, H. *Organometallics* **2002**, *21*, 1326.

(26) Ueno, K.; Nakano, K.; Ogino, H. *Chem. Lett.* **1996**, 459.

(27) Mitchell, G. P.; Tilley, T. D. *Organometallics* **1996**, *15*, 3477.

(28) Mitchell, G. P.; Tilley, T. D. *J. Am. Chem. Soc.* **1998**, *120*, 7635.

(29) Mitchell, G. P.; Tilley, T. D.; Yap, G. P. A.; Rheingold, A. L. *Organometallics* **1995**, *14*, 5472.

(30) Kobayashi, T.; Hayashi, T.; Yamashita, H.; Tanaka, M. *Chem. Lett.* **1988**, 1411.

10.1021/om020389u CCC: \$22.00

$$\underset{X\,=\,Cl,\ OTf}{L_nM{-}SiR_2X} \xrightarrow[-\ M'X]{M'BAr_4} [L_nM{=}SiR_2]^{\oplus}\ [BAr_4]^{\ominus} \qquad (1)$$

$$L_nM \ + \ :SiR_2 \longrightarrow L_mM{=}SiR_2 \qquad (2)$$

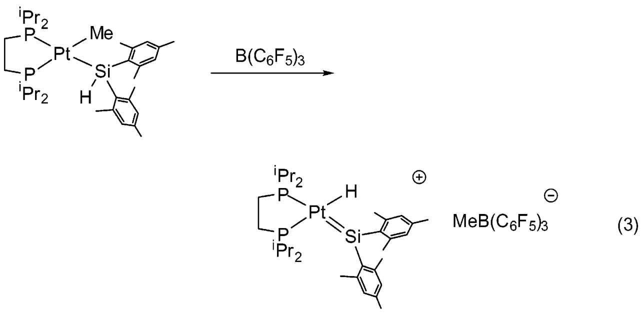

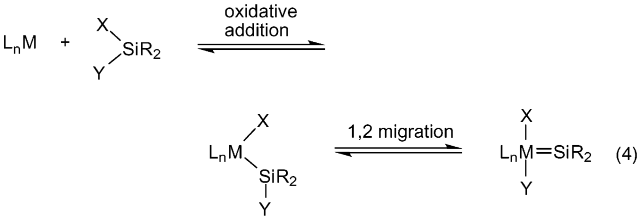

Given the potential for 1,2-migrations to produce reactive silylene complexes that may mediate new chemical transformations, we have sought to develop reaction systems for which this migration is facile. One approach is based on extension of the induced-migration method used to form the four-coordinate Pt(II) silylene complex shown in eq 3 to other metal systems and coordination geometries. An initial goal targeted migrations that would generate stable octahedral complexes, and for this purpose we have focused on d^6 Ir(III). In related work, it has been shown that addition of H_2SiMes_2 to Cp*(PMe_3)IrMe(OTf) (where OTf = OSO_2CF_3) produces the silylene complex [Cp*(PMe_3)(H)Ir=$SiMes_2$][OTf], and mechanistic studies suggested that this transformation occurs via 1,2-migration of hydrogen in the intermediate [Cp*(PMe_3)Ir$SiHMes_2$][OTf].[31]

In this contribution we describe migrations that produce octahedral iridium silylene complexes and a general chemical process that involves the facile extrusion of silylenes and germylenes from secondary silanes and germanes (R_2EH_2: E = Si, Ge). As discussed below, this chemistry appears to involve 1,2-migrations between iridium and silicon (or germanium). Some of these results have been communicated previously.[32] Extrusions of this general type are potentially useful in catalysis and have been identified in a few other cases. For example, extrusions of carbenes from organic substrates have been observed at electron-rich metal centers.[33−41] In addition, the extrusion of a germylene from a germane[42,43] has been reported by Banaszak Holl.

Results and Discussion

An Iridium Silylene Complex via 1,2-Hydrogen Migration. Our strategy for the generation of iridium silylene complexes via migration chemistry targeted a 5-coordinate, 16-electron Ir−$SiHR_2$ derivative. It was envisioned that such a species might be available by methide abstraction, and a suitable starting material proved to be $(Me_3P)_3Ir(SiHMes_2)(Me)(H)$ (**1**), prepared by addition of Mes_2SiH_2 to $(Me_3P)_4IrMe$.[44] Upon addition of $B(C_6F_5)_3$ to **1** in CH_2Cl_2, the reaction solution changed from colorless to yellow, and NMR spectroscopy indicated quantitative formation of a new product (**2**). For **2**, a resonance attributed to $H_3C{-}B(C_6F_5)_3$ (δ 0.52) and an IrH resonance which is integrated as two hydrogens (δ −11.02, $^2J_{HP(trans)} = 84$ Hz) were observed. This suggested that abstraction of Me^- had occurred, followed by a 1,2-H migration from silicon to iridium to form the silylene complex [*fac*-$(Me_3P)_3(H)_2Ir(SiMes_2)$][$MeB(C_6F_5)_3$] (**2**; eq 5). This was verified by the $^{29}Si\{^1H\}$ NMR spectrum of **2**, which contains a large downfield chemical shift (δ 241, dt, $^2J_{SiP(trans)} = 172$ Hz, $^2J_{SiP(cis)} = 4$ Hz), characteristic of sp^2-hybridized silicon.[1,8−12,18,19] Presumably Me^- abstraction generated the unsaturated, five-coordinate intermediate [*fac*-$(Me_3P)_3(H)Ir(SiHMes_2)$][$MeB(C_6F_5)_3$], prior to 1,2-H migration to form the coordinatively saturated silylene complex. Formation of the silylene complex upon addition of $B(C_6F_5)_3$ is rapid (<5 min), and no intermediates were observed at room temperature when the reaction was monitored by ^{31}P NMR spectroscopy.

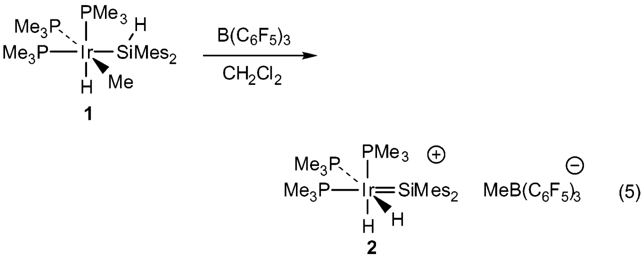

Although analytically pure **2** was easily obtained in powder form by removing the CH_2Cl_2 used in its preparation, we have been unable to crystallize it under a variety of conditions. In general, we have found that crystallizations are often problematic for ionic complexes such as **2**, which contain a fluorocarbon-based anion, $MeB(C_6F_5)_3^-$, and a hydrocarbon-based cation. In an effort to obtain a neutral analogue of **2**, we studied the reactivity of hydrosilanes in a related iridium system based on [$PhBP_3$]Ir(H)(η^3-C_8H_{13})[32] (**3**), where [$PhBP_3$] = $PhB(CH_2PPh_2)_3^-$. This complex contains three facially

---

(31) Klei, S. R.; Tilley, T. D.; Bergman, R. G. *J. Am. Chem. Soc.* **2000**, *122*, 1816.

(32) Peters, J. C.; Feldman, J. D.; Tilley, T. D. *J. Am. Chem. Soc.* **1999**, *121*, 9871.

(33) Empsall, H. D.; Hyde, E. M.; Markham, R.; McDonald, W. S.; Norton, M. C.; Shaw, B. L.; Weeks, B. *Chem. Commun.* **1977**, 589.

(34) Gutierrez-Puebla, E.; Monge, A.; Nicasio, M. C.; Perez, P. J.; Poveda, M. L.; Carmona, E. *Chem. Eur. J.* **1998**, *4*, 2225.

(35) Slugovc, C.; Mereiter, K.; Trofimenko, S.; Carmona, E. *Angew. Chem., Int. Ed.* **2000**, *39*, 2158.

(36) Caulton, K. *J. Organomet. Chem.* **2001**, *617−618*, 56.

(37) Coalter, J. N.; Ferrando, G.; Caulton, K. *New J. Chem.* **2000**, *24*, 835.

(38) Coalter, J. N., III; Huffman, J. C.; Caulton, K. *Chem. Commun.* **2001**, 1158.

(39) Ferrando, G.; Gerard, H.; Spivak, G. J.; Coalter, J. N., III; Huffman, J. C.; Eisenstein, O.; Caulton, K. *Inorg. Chem.* **2001**, *40*, 6610.

(40) Luecke, H. F.; Arndtsen, B. A.; Burger, P.; Bergman, R. G. *J. Am. Chem. Soc.* **1996**, *118*, 2517.

(41) Lee, D.-H.; Chen, J. T.; Faller, J. W.; Crabtree, R. H. *Chem. Commun.* **2001**, 213.

(42) Litz, K. E.; Bender, J. E.; Kampf, J. W.; Banaszak Holl, M. M. *Angew. Chem., Int. Ed. Engl.* **1997**, *36*, 496.

(43) Litz, K. E.; Henderson, K.; Gourley, R. W.; Banaszak Holl, M. M. *Organometallics* **1995**, *14*, 5008.

(44) Thorn, D. L. *Organometallics* **1982**, *1*, 197.

Scheme 1

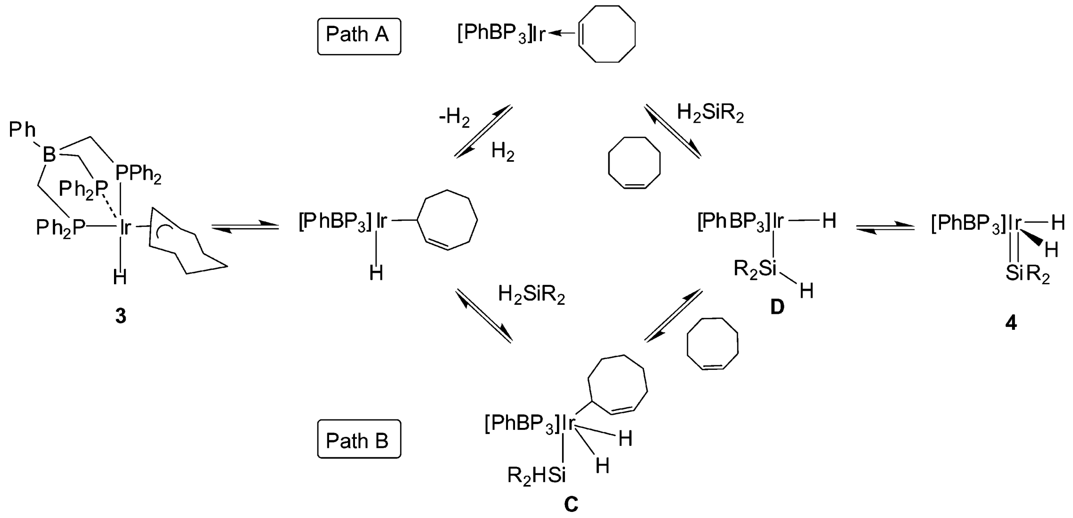

Table 1. ^{29}Si NMR Shifts for the Silylene Complexes $[PhBP_3](H)_2Ir{=}SiR_2$

R_2	^{29}Si NMR, δ	R_2	^{29}Si NMR, δ
Mes_2	241	Me_2	311
Ph_2	327	$Mes(C_8H_{15})$	274
Et_2	307	$Trip(C_8H_{15})$	317

coordinated phosphines but is zwitterionic, with a borate incorporated into the ligand backbone.

Silylene Extrusion from Secondary Silanes. Complex **3** reacts with secondary silanes (H_2SiR_2, with R = Mes, Ph, Et, Me) in benzene to give silylene dihydride complexes of the type $[PhBP_3](H)_2Ir{=}SiR_2$ (eq 6: R = Mes, **4a**; R = Ph, **4b**; R = Et, **4c**; R = Me, **4d**), with concomitant loss of cyclooctene (COE). Formation of the silylene complex was confirmed by $^{29}Si\{^1H\}$ NMR spectroscopy, as all the complexes exhibit resonances downfield of 200 ppm (Table 1). The required reaction conditions varied depending on the steric bulk of the silane. For example, in benzene-d_6, formation of $[PhBP_3](H)_2Ir{=}SiMes_2$ required heating at 95 °C for 24 h while $[PhBP_3](H)_2Ir{=}SiMe_2$ formed after heating at 80 °C for 2 min. Furthermore, formation of the silylene complex is nearly complete in each case (>85% by NMR spectroscopy). This transformation is exceptional in that the direct conversion of secondary silanes to silylene complexes was previously unknown.

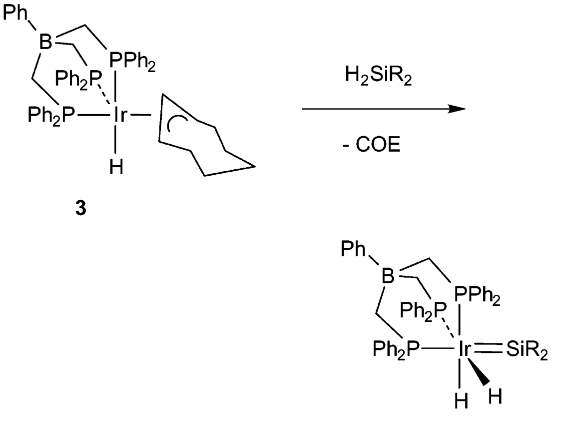

(6)

R = Mes (**4a**), Ph (**4b**), Et (**4c**), Me (**4d**)

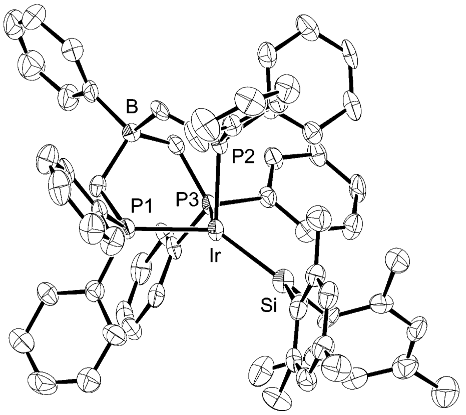

Figure 1. ORTEP diagram of $[PhBP_3](H)_2Ir{=}SiMes_2$ (**4a**).

Interestingly, the related parent allyl complex $[PhBP_3]Ir(H)(\eta^3\text{-}C_3H_5)$[45] did not react with R_2SiH_2 (R = Mes, Et, or Me) under forcing conditions (benzene-d_6, 80 °C, 1 week). The inertness of this complex relative to **3** may reflect a reduced tendency for it to undergo a change in hapticity (η^3 to η^1; Scheme 1) which would allow oxidative addition to the metal center. It is also noteworthy that the related complexes $TpIr(H)(\eta^3\text{-}C_8H_{13})$[46] and $Tp^{Me_2}Ir(H)(\eta^3\text{-}C_4H_7)$[46] (where Tp = hydridotris(pyrazolyl)borate and Tp^{Me_2} = hydridotris(3,5-dimethylpyrazolyl)borate), which are less electron-rich and less sterically demanding than **3**,[45] fail to react with H_2SiMes_2 (benzene-d_6, 92 °C, 24 h).

The dimesitylsilylene complex $[PhBP_3](H)_2Ir{=}SiMes_2$ (**4a**) was precipitated by the addition of pentane to a toluene solution of **4a** (67% yield). The molecular structure of **4a** (Figure 1) features a dimesitylsilylene ligand which is planar at silicon (sum of the angles about Si 359.0(6)°). Notably, the Ir=Si bond distance of 2.260(3) Å is 5% shorter than the average of previously observed Ir−Si distances (2.39 Å).[47] The $[PhBP_3]$ ligand is facially coordinated to iridium with P−Ir−P angles

---

[45] Feldman, J. D.; Peters, J. C.; Tilley, T. D. *Organometallics*, in press.

[46] Alvarado, Y.; Boutry, O.; Gutierrez, E.; Monge, A.; Nicasio, M. C.; Poveda, M. L.; Perez, P. J.; Ruiz, C.; Bianchini, C.; Carmona, E. *Chem. Eur. J.* **1997**, *3*, 860.

[47] Corey, J. Y.; Braddock-Wilking, J. *Chem. Rev.* **1999**, *99*, 175.

Table 2. Crystallographic Data for 4a, 5, and 6

	4a	**5**	**6**
empirical formula	$C_{72}H_{71}BP_3IrOSi$	$C_{47}H_{49}BP_3IrOSi_2$	$C_{75}H_{75}BP_3IrGe$
fw	1268.39	1837.76	1344.99
cryst size (mm)	0.05 × 0.21 × 0.30	0.12 × 0.10 × 0.02	0.34 × 0.10 × 0.03
cryst syst	monoclinic	monoclinic	monoclinic
space group	$P2_1/c$	$P2_1/n$	$P\bar{1}$
a (Å)	11.5877(2)	15.956(1)	13.2680(7)
b (Å)	19.6433(2)	28.838(2)	14.1823(7)
c (Å)	27.2469(5)	18.279(1)	19.105(1)
α (deg)	90	90	88.229(1)
β (deg)	91.569(1)	92.025(1)	73.711(2)
γ (deg)	90	90	66.383(2)
V (Å^3)	6199.6(2)	8406(2)	3148.1(3)
orientation rflns: no., 2*θ* range (deg)	6753, 3.0−45.0	4517, 3.0−46.0	2730, 3.0−46.0
Z	4	8	2
D_{calcd} (g/cm^3)	1.359	1.552	1.269
diffractometer	SMART		
radiation	Mo Kα ($\lambda = 0.710\ 69$ Å), graphite monochromated		
temp (K)	167(1)	140(1)	155(1)
scan type	*ω* (0.3° per frame)		
scan rate (s/frame)	10.0		
data collected, $2\theta_{max}$ (deg)	49.4	51.2	51.3
no. of rflns measd			
total	10 766	38 028	15 973
unique	5890	14 426	10 012
R_{int}	0.075	0.100	0.062
structure soln	direct methods (SIR92)		
no. of obsd data ($I > 3\sigma(I)$)	5890	4956	4392
no. of params refined	665	534	350
final residuals: *R*; R_w; R_{all}[a]	0.047; 0.049; 0.106	0.034; 0.032; 0.034	0.041; 0.040; 0.111
goodness of fit indicator[b]	1.54	0.82	0.89
max. shift/error final cycle	0.04	0.08	0.01
max and min peaks, final diff map (e/Å^3)	1.63, −1.15	0.97, −0.63	1.27, −0.88

[a] $R = \sum||F_o| - |F_c||/\sum|F_o|$; $R_w = [\sum w(|F_o| - |F_c|)^2/\sum wF_o^2]^{1/2}$. [b] Goodness of fit $= [\sum w(|F_o| - |F_c|)^2/(N_{observns} - N_{params})]^{1/2}$.

Table 3. Selected Bond Distances (Å) and Angles (deg) for 4a

(a) Bond Distances			
Ir1−P1	2.345(3)	Ir1−P3	2.408(2)
Ir1−P2	2.329(3)	Ir1−Si1	2.260(3)
(b) Bond Angles			
P1−Ir1−P2	90.84(9)	P1−Ir1−Si1	141.5(1)
P1−Ir1−P3	89.11(8)	P2−Ir1−Si1	120.9(1)
P2−Ir1−P3	86.17(9)	P3−Ir1−Si1	112.32(9)

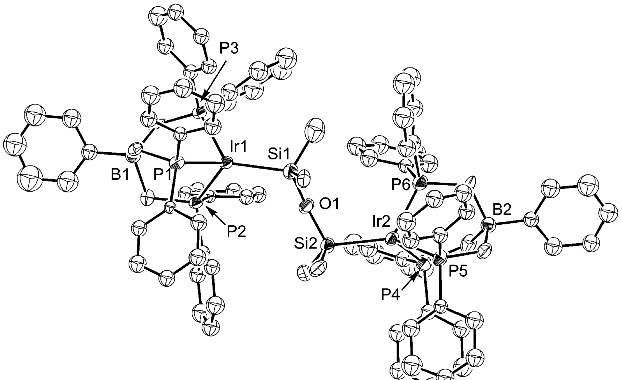

Figure 2. ORTEP diagram of {[PhBP$_3$](H)$_3$IrSiMe$_2$}$_2$O (**5**).

of 86−91°, but otherwise the iridium center is distorted from ideal octahedral geometry. Significant steric interactions between dimesitylsilylene and the bulky [PhBP$_3$] ligand presumably give rise to the Si−Ir−P angles of 141.5(1), 120.9(1), and 112.3(1)° (vs 180, 90, and 90° for an ideal octahedron). Selected bond distances and angles for **4a** are listed in Table 3.

Except for **4a**, which possesses the most sterically demanding substituents at silicon, these silylene complexes are thermally unstable. For **4b-4d**, removal of the solvent in vacuo resulted in significant decomposition (>50%) to mixtures of products. For [PhBP$_3$](H)$_2$-Ir=SiMe$_2$ (**4d**) an apparent hydrolysis product was observed when crystals were grown over several weeks from a toluene solution which had been layered with Et$_2$O. Analysis of these crystals by X-ray crystallography revealed the bimetallic complex {[PhBP$_3$](H)$_3$Ir(SiMe$_2$)}O (**5**, Figure 2 and Table 4), which is assumed to be the result of slow diffusion of adventitious water into the solution of **4d** (eq 7). Attempts to prepare **5** via the stoichiometric addition of H$_2$O to **4d** in benzene-d_6 gave a mixture of products.

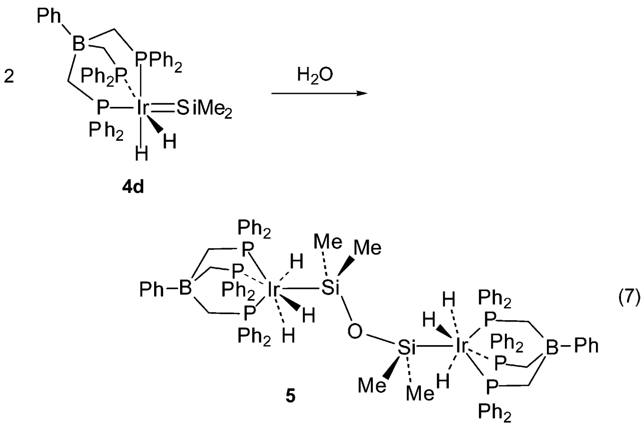

Germylene Extrusion from a Germane. Given the generality of the transformation shown in eq 6, we attempted to extend this method to the formation of germylene complexes from secondary germanes. The reaction of Mes$_2$GeH$_2$ with **3** (benzene, 83 °C, 36 h) gave

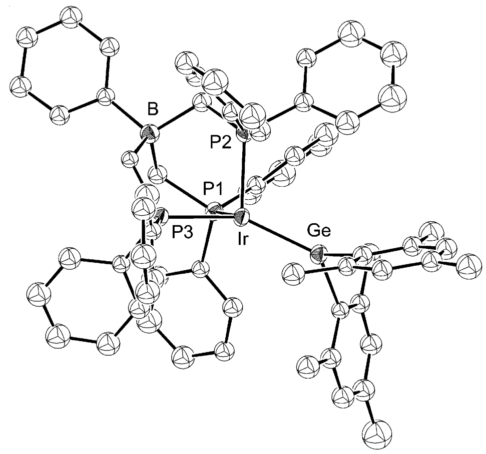

Figure 3. ORTEP diagram of $[PhBP_3](H)_2Ir{=}GeMes_2$ (**6**).

Table 4. Selected Bond Distances (Å) and Angles (deg) for 5

(a) Bond Distances			
Ir1−P1	2.353(3)	Ir1−Si1	2.408(4)
Ir1−P2	2.358(3)	Si1−O1	1.637(8)
Ir1−P3	2.358(3)	Si2−O1	1.646(8)
(b) Bond Angles			
P1−Ir1−Si1	133.4(1)	P3−Ir2−Si2	124.8(1)
P2−Ir1−Si1	117.3(1)	P4−Ir2−Si2	125.8(1)
P3−Ir1−Si1	124.8(1)	P5−Ir2−Si2	126.6(1)
Ir1−Si1−O1	112.8(3)	Ir2−Si2−O1	111.9(3)
Si1−O1−Si2	148.6(6)		

Table 5. Selected Bond Distances (Å) and Angles (deg) for 6

(a) Bond Distances			
Ir1−P1	2.362(3)	Ir1−P3	2.310(3)
Ir1−P2	2.329(3)	Ir1−Ge1	2.339(1)
(b) Bond Angles			
P1−Ir1−P2	91.9(1)	P1−Ir1−Ge1	111.02(7)
P1−Ir1−P3	88.1(1)	P2−Ir1−Ge1	113.59(8)
P2−Ir1−P3	90.2(1)	P3−Ir1−Ge1	147.96(8)

$[PhBP_3](H)_2Ir{=}GeMes_2$ (**6**), which was isolated in 76% yield. Like the analogous silylene complexes, the $^{31}P\{^1H\}$ NMR spectrum of **6** consists of two coupled resonances (benzene-d_6, δ 6.12, 3.61, $^2J_{PP} = 19$ Hz), and the ^1H NMR spectrum features an IrH resonance (δ −9.68, dm, $^2J_{HPtrans} = 83$ Hz) which is integrated as two hydrogens. Complex **3** did not give analogous stannylene or carbene complexes upon addition of secondary stannanes or alkanes; H_2CR_2 (R = Ph, Mes) failed to react with **3** in benzene-d_6 after heating at 95 °C for 2 weeks, and Mes_2SnH_2 reacted immediately with **3** in benzene-d_6 at room temperature to give a variety of iridium products, H_2, and several Sn−H-containing compounds (by ^1H NMR spectroscopy).

X-ray-quality crystals of **6** were grown via the slow evaporation of a benzene-d_6 solution; an ORTEP diagram is shown in Figure 3, and selected bond distances and angles are given in Table 5. Germylene complex **6** is structurally similar to its silylene analogue (**4a**). The dimesitylgermylene substituent is bent away from the bulky $[PhBP_3]$ phosphine groups, resulting in Ge−Ir−P angles of 147.96(8), 113.59(8), and 111.02(7)°. The germanium coordination plane (Ir, Ge, C, C) is nearly trigonal planar, with the sum of the angles about Ge being 355.7(6)°, and the Ir=Ge bond distance is 2.339(1) Å. The only other crystallographically characterized complexes containing Ge−Ir bonds are $(Ph_3P)_2(CO)(H)_2IrGeMe_3$[48] and the germylene complexes **A** and **B**.[49]

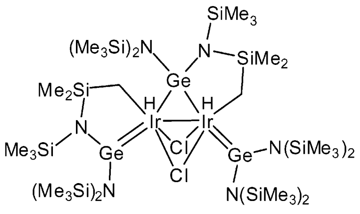

A

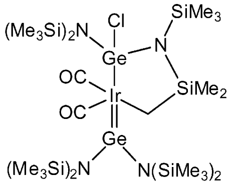

B

Among these structures, the Ge−Ir distances range from 2.32 to 2.47 Å, with the shorter distances corresponding to germylene−iridium contacts.

Mechanistic Considerations for Silylene Extrusion from Secondary Silanes. Two possible mechanisms for silylene (or germylene) formation from the reactions of H_2SiR_2 (or H_2GeR_2) with $[PhBP_3]Ir(H)(\eta^3\text{-}C_8H_{13})$ are shown in Scheme 1. In path A, an η^1-allyl complex is in equilibrium with an η^2-COE complex, and addition of an Si−H bond followed by loss of cyclooctene would yield the 16-electron silyl intermediate **D**. This unsaturated intermediate would then undergo 1,2-H migration to form the observed silylene product, in which iridium is coordinatively and electronically saturated. Alternatively, as shown in path B, **3** could be in equilibrium with an η^1-allyl complex, which then undergoes oxidative addition of H_2SiR_2 to give an Ir(V) intermediate (**C**). From this intermediate, reductive elimination of COE and 1,2-H migration would produce the final product.

In an effort to determine which mechanism is operative, the reaction of **3** with D_2SiMes_2 was monitored by NMR spectroscopy. While path A would yield a product with two iridium deuterides, $[PhBP_3](D)_2Ir{=}SiMes_2$, path B would give a mixture of deuteride and hydride ligands in the iridium product, with some of the deuterium label being incorporated into cyclooctene. To our surprise, this labeling study did not lead to products consistent with path A or B but instead revealed the presence of a $[PhBP_3]$ ligand metalation process.

During the course of a reaction of D_2SiMes_2 with **3** (benzene, 80 °C, 3 h) the deuterium label was incorporated into the ortho position of the *P*-phenyl substituent of $[PhBP_3]$ as well as various positions of the C_8H_{13} ring of **3** prior to product formation (by ^1H, $^2H\{^1H\}$, and $^{31}P\{^1H\}$ NMR spectroscopy). This observation indicates that silane addition to $[PhBP_3]Ir(H)(\eta^3\text{-}C_8H_{13})$ is reversible (D_2SiMes_2 is converted to H_2SiMes_2 prior to formation of the silylene complex), that ortho metalation of the ligand *P*-phenyl groups is a rapid, reversible process,

---

[48] Bell, N. A.; Glockling, F.; Schneider, M. L.; Shearer, H. M. M.; Wibley, M. D. *Acta Crystallogr. Sect. C: Cryst. Struct. Commun.* **1984**, *40*, 625.

[49] Hawkins, S. M.; Hitchcock, P. B.; Lappert, M. F.; Rai, A. K. *Chem. Commun.* **1986**, 1689.

and that exchange of iridium-bound and cyclooctenyl-bound hydrogens occurs rapidly (eq 8).[50] The metalation process is consistent with our recent observation of the ortho-metalation product $\{PhB[(CH_2PPh_2)_2(CH_2PPh\text{-}C_6H_4)]\}Ir(H)(PMe_3)$, which forms upon addition of PMe_3 to **3**.[45]

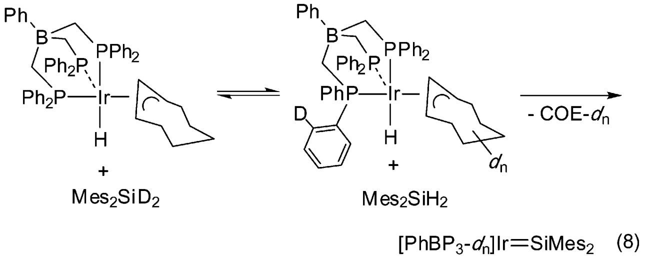

(8)

We have observed evidence to suggest that the hydride ligands readily migrate back to silicon. For example, the addition of excess CO to **4a** (benzene-d_6, 92 °C, 24 h) produced Mes_2SiH_2 and $[PhBP_3]Ir(CO)_2$ (quantitative by $^{31}P\{^1H\}$ NMR spectroscopy). Additionally, a C−H activation process was observed upon reaction of propene with **4a** (1 atm, benzene-d_6, 80 °C). After 7 days at 80 °C, 40% conversion to Mes_2SiH_2 and $[PhBP_3]Ir(H)(\eta^3\text{-}C_3H_5)$ was observed (eq 9). This first example of a C−H activation by a transition silylene complex suggests that silylene complexes derived from $[PhBP_3]Ir$ may possess a rich reaction chemistry.

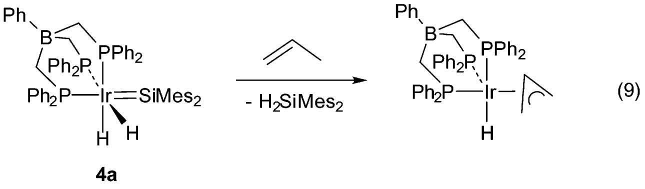

(9)

Activation of Tertiary Silanes. Both mechanisms in Scheme 1 involve a rearrangement of the 16-electron silyl intermediate **D** to an 18-electron silylene species via 1,2-H migration from silicon to iridium. This migration should be less favorable for substituents other than H, and thus we studied the reactions of tertiary silanes ($HSiR_3$) with $[PhBP_3]Ir(H)(\eta^3\text{-}C_8H_{13})$ (**3**) in an effort to observe silyl complexes analogous to the proposed intermediates **C** and **D**. However, as described below, reactions of **3** with tertiary silanes are not analogous to those with secondary silanes. For example, thermolysis of **3** with 1 equiv of $HSiEt_3$ (benzene-d_6, 60 °C, 20 h) led to formation of 1,3-cyclooctadiene (by GC/MS), and by ^1H NMR spectroscopy an IrH resonance which is integrated as three hydrogens (δ −10.6, $^2J_{HP}$ = 81 Hz) and a triethylsilyl substituent are observed. Additionally, the phosphine ligands are equivalent by $^{31}P\{^1H\}$ NMR spectroscopy (δ −3.81). These data are consistent with the symmetrical, silyl-capped Ir(V) species $[PhBP_3]IrH_3(SiEt_3)$ (**7a**, eq 10). This reaction was quantitative by ^1H and $^{31}P\{^1H\}$ NMR spectroscopy; the isolated yield of **7a** was 38%. It is interesting to note that, depending on reaction conditions, complex **3** may behave as a source of "$[PhBP_3]Ir$" (with elimination of COE as a byproduct, as in the reactions with secondary silanes) or as a source of "$[PhBP_3]IrH_2$" (with elimination of 1,3-COD, as in the reactions with tertiary silanes). This difference has also been observed in reactions of **3** with phosphines.[45] As yet, we do not fully understand the factors that influence this reactivity.

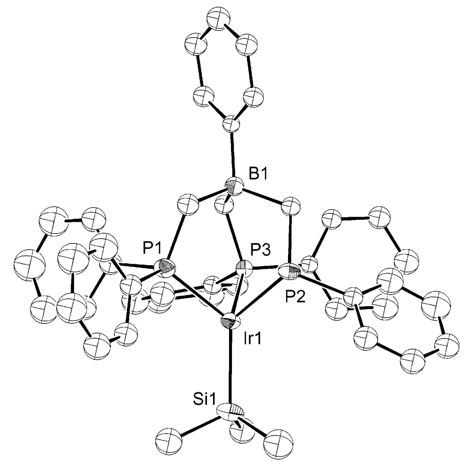

Figure 4. ORTEP diagram of one of the two crystallographically independent molecules of $[PhBP_3]IrH_3(SiMe_3)$ (**7b**). One of the phenyl groups on P2 has been omitted for clarity.

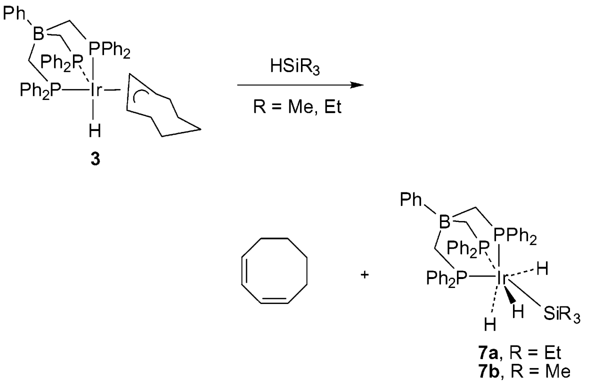

(10)

Under an atmosphere of $HSiMe_3$ **3** reacts (benzene, 75 °C, 6 days) to give the corresponding trimethylsilyl product $[PhBP_3]IrH_3(SiMe_3)$ (**7b**), which was isolated in 66% yield. The NMR data for **7b** are quite similar to those of **7a**, which suggests that the complexes are isostructural in solution. The solid-state structure of **7b** was determined by X-ray crystallography (Figure 4) and confirms the geometry of this complex, which may be described as a distorted, silyl-capped octahedron. Two structurally similar molecules are in the asymmetric unit. In both molecules all P−Ir−P angles are approximately 90°, while the P−Ir−Si angles range from 119 to 129°. Selected bond distances and angles for **7b** are given in Table 7. Overall, the coordination geometry for iridium is similar to that in the related complex $Tp^{Me_2}IrH_3(SiEt_3)$.[51] However, it contrasts with the structures of related Cp* complexes, including $Cp^*IrH_3(ER_3)$ (where ER_3 = $SiMe_3$, $SnMe_3$, $SnPh_3$)[52] and $Cp^*IrH_2(SiEt_3)_2$,[53] which may be described as four-legged piano stools.

---

[50] Two reversible processes to account for this are feasible: insertion of COE into the Ir−H bond, or β-H elimination to form $[PhBP_3]Ir(H)_2(COD)$, where COD = 1,3-cyclooctadiene.

[51] Gutierrez-Puebla, E.; Monge, A.; Paneque, M.; Poveda, M. L.; Taboada, S.; Trujillo, M.; Carmona, E. *J. Am. Chem. Soc.* **1999**, *121*, 346.

Table 6. Crystallographic Data for 7b and 8a

	7b	8a
empirical formula	$C_{48}H_{50}BP_3IrSi$	$C_{62}H_{69}BP_3IrSi$
fw	994.05	985.98
cryst size (mm)	0.19 × 0.16 × 0.07	0.30 × 0.25 × 0.07
cryst syst	triclinic	monoclinic
space group	$P\bar{1}$	$P2_1/c$
a (Å)	13.3907(3)	16.9431(4)
b (Å)	17.3646(4)	14.9301(1)
c (Å)	20.4662(3)	21.3674(4)
α (deg)	65.825(1)	90
β (deg)	86.788(2)	99.521(1)
γ (deg)	89.680(2)	90
V (Å^3)	4333.9(2)	5330.7(2)
orientation rflns: no., 2θ range (deg)	3923, 3.0−45.0	6301, 3.0−45.0
Z	4	4
D_{calcd} (g/cm^3)	1.523	1.228
diffractometer	SMART	
radiation	Mo Kα ($\lambda = 0.710\ 69$ Å), graphite monochromated	
temp (K)	154(1)	
scan type	ω (0.3° per frame)	
scan rate (s/frame)	10.0	
no. of data collected, $2\theta_{max}$ (deg)	46.5	
no. of rflns measd		
total	25 520	24 769
unique	14 104	7975
R_{int}	0.056	0.100
structure soln	direct methods (SIR92)	
no. of obsd data ($I > 3\sigma(I)$)	5626	4387
no. of params refined	483	592
final residuals: R; R_w; R_{all}[a]	0.035; 0.035; 0.108	0.037; 0.038; 0.081
goodness of fit indicator[b]	0.84	1.34
max shift/error final cycle	0.00	0.01
max and min peaks, final diff map (e/Å^3)	1.47, −0.53	0.67, −0.39

[a] $R = \sum||F_o| - |F_c||/\sum|F_o|$; $R_w = [\sum w(|F_o| - |F_c|)^2/\sum wF_o^2]^{1/2}$. [b] Goodness of fit $= [\sum w(|F_o| - |F_c|)^2/(N_{observns} - N_{params})]^{1/2}$.

Table 7. Selected Bond Distances (Å) and Angles (deg) for 7b

(a) Bond Distances			
Ir1−P1	2.367(3)	Ir1−P3	2.375(3)
Ir1−P2	2.363(3)	Ir1−Si1	2.437(3)
(b) Bond Angles			
P1−Ir1−P2	89.7(1)	P1−Ir1−Si1	128.5(1)
P1−Ir1−P3	91.6(1)	P2−Ir1−Si1	128.1(1)
P2−Ir1−P3	88.9(1)	P3−Ir1−Si1	118.7(1)

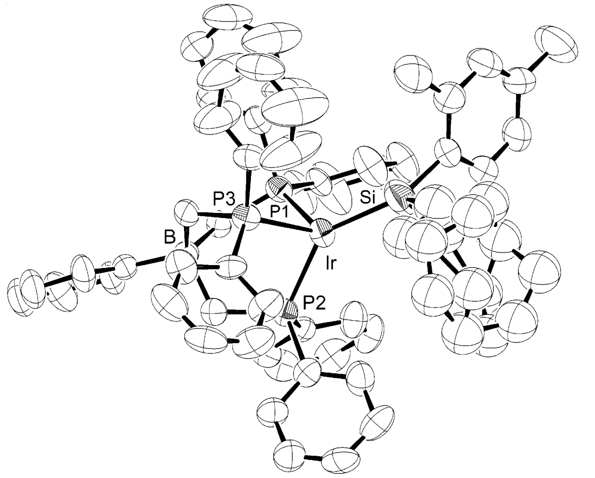

Figure 5. ORTEP diagram of $[PhBP_3](H)_2Ir{=}Si(Mes)(c\text{-}C_8H_{15})$ (**8a**). The cyclooctyl ring bound to silicon is highly disordered, and several partial-occupancy carbon atoms are displayed.

Table 8. Selected Bond Distances (Å) and Angles (deg) for 8a

(a) Bond Distances			
Ir1−P1	2.377(2)	Ir1−P3	2.328(2)
Ir1−P2	2.333(2)	Ir1−Si1	2.250(3)
(b) Bond Angles			
P1−Ir1−P2	87.98(8)	P1−Ir1−Si1	115.3(1)
P1−Ir1−P3	88.51(8)	P2−Ir1−Si1	140.7(1)
P2−Ir1−P3	90.43(8)	P3−Ir1−Si1	119.7(1)

Scheme 2

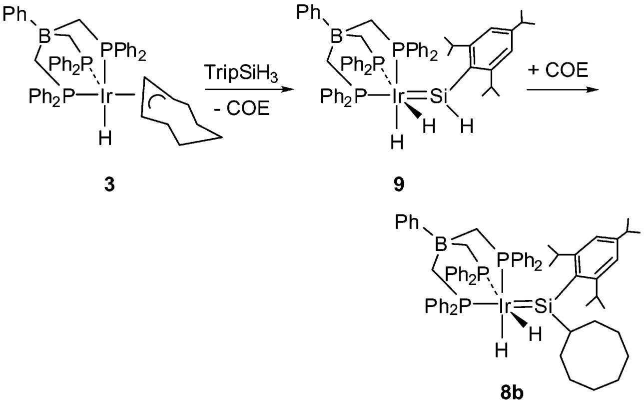

Silylene Complexes Derived from Primary Silanes. Given the ease with which silylenes are extruded from secondary silanes using **3**, we sought to prepare complexes with a hydrogen substituent on the silylene ligand, $[PhBP_3](H)_2Ir{=}SiH(R)$, from the reaction of **3** with primary silanes. Such species are expected to be quite reactive, given the presence of a Si−H bond and the relatively low steric protection for the silylene center. Recently a silylene complex of this type, $[(Et_3P)_3(H)_2Ir{=}SiH(C_6H_3Mes_2\text{-}2,6)][B(C_6F_5)]$, was reported.[54]

The reaction of $MesSiH_3$ with **3** (benzene-d_6, 25 °C, 24 h) did in fact cleanly produce a new species with a $^{29}Si\{^1H\}$ NMR shift of δ 274, consistent with the formation of a silylene complex. However, by ^1H NMR spectroscopy no resonances consistent with COE or the presence of a Si−H bond were observed. Instead, several methylene resonances (δ 1.73−2.03) were observed, suggesting the possibility of a cyclooctyl substituent on silicon and a silylene complex of the type $[PhBP_3](H)_2Ir{=}Si(Mes)(c\text{-}C_8H_{15})$ (**8a**). Such a product could result (formally) from the hydrosilylation of COE by the anticipated silylene complex, $[PhBP_3](H)_2Ir{=}SiH(Mes)$.

An X-ray diffraction study of complex **8a** confirmed its structure (Figure 5), which is similar to that of **4a**. The Ir═Si bond distance of 2.250(3) Å is the shortest Ir−Si contact reported to date.[55] The geometry at iridium is a distorted octahedron, with P−Ir−P angles ranging from 88 to 90° and P−Ir−Si angles of 140.7(1),

---

(52) Gilbert, T. M.; Hollander, F. J.; Bergman, R. G. *J. Am. Chem. Soc.* **1985**, *107*, 3508.

(53) Ricci, J. S., Jr.; Koetzle, T. F.; Fernandez, M. J.; Maitlis, P. M.; Green, J. C. *J. Organomet. Chem.* **1986**, *299*, 383.

(54) Simmons, R. S.; Gallucci, J. C.; Tessier, C. A.; Youngs, W. J. *J. Organomet. Chem.* **2002**, *654*, 224.

(55) Based on a search of the Cambridge Structural Database, April 2002.

Scheme 3

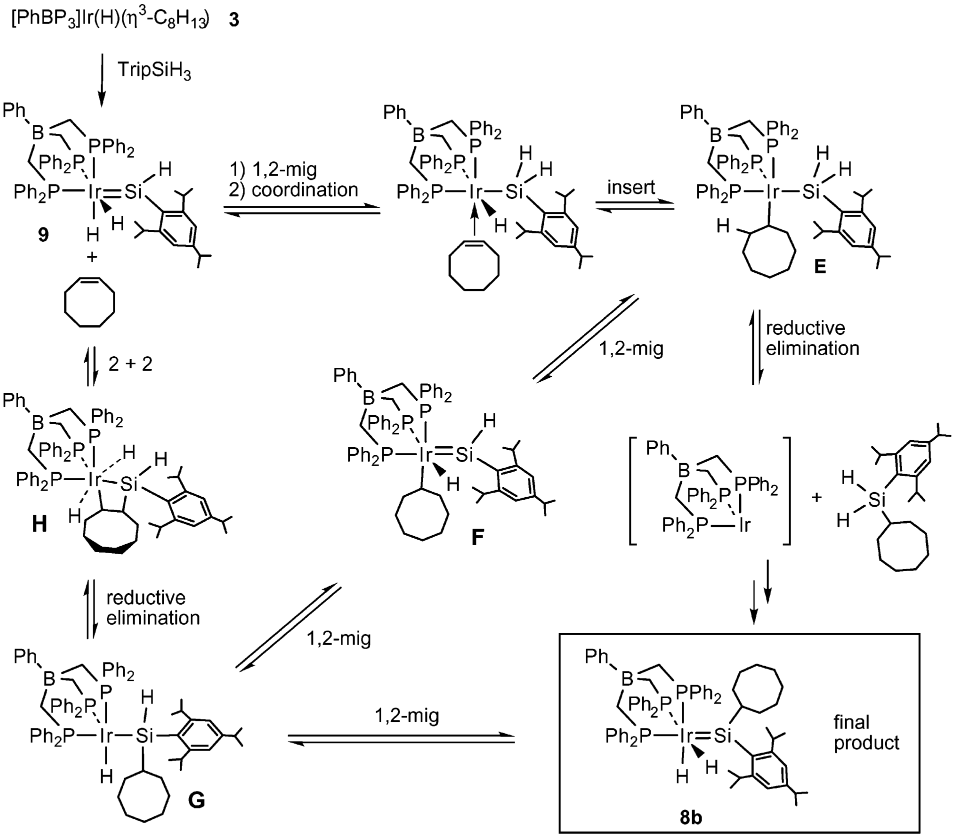

119.7(1), and 115.3(1)°. Significantly, the crystallographic data are consistent with the presence of a cyclooctyl substituent on the silylene moiety, which confirms that activation of all three Si−H bonds of $\mathrm{MesSiH_3}$ has taken place. Additional bond distances and angles for **8a** are listed in Table 8.

In a reaction of the more sterically congested 2,4,6-triisopropylphenylsilane ($\mathrm{TripSiH_3}$) with **3** (toluene, room temperature, 2.5 days), an intermediate was observed in the course of an analogous triple Si−H bond activation. As in the case above, a cyclooctylsilylene complex, $[\mathrm{PhBP_3}](\mathrm{H})_2\mathrm{Ir{=}Si(Trip)}(c\text{-}\mathrm{C_8H_{15}})$ (**8b**), is the final product with a $^{29}\mathrm{Si}\{^1\mathrm{H}\}$ NMR resonance of δ 317. However, when the reaction was monitored by NMR spectroscopy, intermediate formation of COE and a species consistent with $[\mathrm{PhBP_3}](\mathrm{H})_2\mathrm{Ir{=}SiH(Trip)}$ (**9**) was observed (Scheme 2). The concentration of **9** did not build up significantly (<20%), but it was observed in the presence of COE and was completely converted to **8b** once all of the COE had been consumed. For **9**, two coupled resonances are observed by $^{31}\mathrm{P}\{^1\mathrm{H}\}$ NMR spectroscopy (δ 2.87 and 1.86, $^2J_{\mathrm{PP}} = 18$ Hz). The ^{1}H NMR spectrum for silylene **9** features an IrH resonance at δ −9.34 ($^2J_{\mathrm{HPtrans}} = 75$ Hz) and, significantly, a SiH resonance at δ 11.16 ($^3J_{\mathrm{HP}} = 20$ Hz). This downfield shift for the silylene SiH is consistent with $[(\mathrm{Et_3P})_3(\mathrm{H})_2\mathrm{Ir{=}SiH(C_6H_3Mes_2\text{-}2,6)}][\mathrm{B(C_6F_5)}]$[54] and other SiH silylene complexes prepared in our group[56] and is reminiscent of the downfield ^{1}H NMR shifts that have been observed for hydrogen-substituted carbene complexes of the type $\mathrm{L}_n\mathrm{M{=}CHR}$.[57,58]

As outlined in Scheme 3, there are three mechanisms whereby the intermediate $[\mathrm{PhBP_3}](\mathrm{H})_2\mathrm{Ir{=}SiH(Trip)}$ (**9**) can react with COE to give the final product $[\mathrm{PhBP_3}](\mathrm{H})_2\mathrm{Ir{=}SiH(Trip)}$ (**8b**). First, 1,2-H migration from silicon to iridium followed by COE coordination, and migratory insertion would generate five-coordinate $[\mathrm{PhBP_3}]\mathrm{Ir}(c\text{-}\mathrm{C_8H_{15}})(\mathrm{SiH_2Trip})$ (**E**). Intermediate **E** could undergo reductive elimination to give $\mathrm{H_2Si(Trip)}(c\text{-}\mathrm{C_8H_{15}})$ and "$[\mathrm{PhBP_3}]\mathrm{Ir}$",[59] which could then form the product silylene complex **9** via double Si−H activation. Alternatively, intermediate **E** could undergo a series of 1,2-migrations to give silylene complex **F** and silyl complex **G** prior to product formation. Finally, silylene complex **9** could undergo 2 + 2 cycloaddition to give the iridasilacycle **H**; C−H reductive elimination would then generate $[\mathrm{PhBP_3}](\mathrm{H})\mathrm{Ir}(c\text{-}\mathrm{C_8H_{15}})(\mathrm{SiHTrip})$ (**G**), and a 1,2-migration would yield **8b**. Although no 2 + 2 cycloadditions between alkenes and silylene complexes have been reported, products apparently derived from alkyne cycloaddition with silylene complexes have been observed.[2,3,60−65]

---

[56] Several silylene complexes with Si−H bonds have been prepared in our laboratory. These fully characterized complexes exhibit downfield SiH shifts by ^{1}H NMR spectroscopy (δ 10−13). Glaser, P. B.; Mork, B. V.; Tilley, T. D. Manuscripts in preparation.

[57] Guggenberger, L. J.; Schrock, R. R. *J. Am. Chem. Soc.* **1975**, *97*, 6578.

[58] Schwab, P.; Grubbs, R. H.; Ziller, J. W. *J. Am. Chem. Soc.* **1996**, *118*, 100.

[59] "$[\mathrm{PhBP_3}]\mathrm{Ir}$" would more likely exist as a metalated isomer.

[60] Yamamoto, K.; Okinoshi, H.; Kumada, M. *J. Organomet. Chem.* **1971**, *27*, C31.

[61] Yamashita, H.; Tanaka, M.; Goto, M. *Organometallics* **1992**, *11*, 3227.

[62] Seyferth, D.; Shannon, M. L.; Vick, S. C.; Lim, T. F. O. *Organometallics* **1985**, *4*, 57.

[63] Okinoshi. H.; Yamamoto, K.; Kumada, M. *J. Am. Chem. Soc.* **1972**, *94*, 9263.

[64] Sakurai, H.; Kamiyama, Y.; Nakadaira, Y. *J. Am. Chem. Soc.* **1977**, *99*, 3879.

[65] Tanaka, Y.; Yamashita, H.; Tanaka, M. *Organometallics* **1995**, *14*, 530.

Conclusion

In the study described here, migration chemistry in iridium silyl complexes was exploited to produce stable, isolable silylene complexes. The synthetic routes employed have targeted silylene complexes with the most stable coordination geometry for Ir(III), which is designed to form via 1,2-H migration in a reactive, 5-coordinate intermediate. The viability of this approach was first demonstrated by a reaction scheme that appears to generate the 16-electron intermediate $(Me_3P)_3(H)Ir-SiHMes_2^+$, which rapidly converts to the 6-coordinate silylene complex $(Me_3P)_3(H)_2Ir{=}SiMes_2^+$ (**2**). This result, along with those reported earlier for the platinum system of eq 3,[19] emphasizes the importance of changes in the metal's coordination geometry in influencing migration chemistry. Evidently, 1,2-migrations are not favored in square-planar Pt(II) silyl complexes[18,19] or in octahedral Rh(III) silyl complexes.[66] However, reaction schemes that produce less stable coordination geometries (e.g., 3-coordinate Pt(II) or 5-coordinate Ir(III)) can lead to migrations of this type. Such low-coordinate intermediate species may result from ligand abstractions, as reported here and elsewhere,[19,31] but may also form via ligand dissociation processes. This latter possibility is yet to be demonstrated, however.

Further development of this migration chemistry might lead to useful catalytic transformations involving reactive silylene complexes as intermediates. Significant progress in this direction has been made with identification of reactions that involve the facile extrusion of silylene ligands from simple secondary and primary silanes. Notably, this chemistry resulted from investigation of a new iridium-based fragment involving the anionic triphosphine ligand $[PhBP_3]$. With development of new chemical transformations for silylene complexes, it may prove possible to design catalytic cycles that involve silylene extrusions. In this context, it is worth noting the propene reaction of eq 9, which represents the first example of a C−H activation mediated by a transition metal silylene complex. Currently, the mechanism of this conversion is not known. Future efforts will address this issue and the reactivity of silylene complexes toward various organic compounds.

Experimental Section

General Considerations. All experiments were performed under dry nitrogen using standard Schlenk or drybox techniques. Solvents were distilled under nitrogen from sodium benzophenone ketyl, and dichloromethane was distilled from CaH_2. To remove olefin impurities, pentane and benzene were pretreated with concentrated H_2SO_4, 0.5 N $KMnO_4$ in 3 M H_2SO_4, $NaHCO_3$, and then anhydrous $MgSO_4$. Benzene-d_6 and THF-d_8 were distilled from Na/K alloy. Other chemicals were obtained from commercial suppliers and were used as received. $[PhBP_3]Ir(\eta^3\text{-}C_8H_{13})(H)$,[32] $(PMe_3)_4IrMe$,[44] Mes_2SiH_2,[67] and Mes_2GeH_2[68] were prepared according to literature procedures. $TripSiH_3$ was prepared by reaction of $TripSiCl_3$[69] with $LiAlH_4$. Elemental analyses were performed by the Microanalytical Laboratory in the College of Chemistry at the University of California, Berkeley. FT-infrared spectra were recorded on a Mattson FTIR 3000 instrument.

NMR Measurements. Routine ^1H, $^{31}P\{^1H\}$, and $^{13}C\{^1H\}$ NMR spectra were recorded at 298 K on a Bruker DRX-500 instrument equipped with a 5 mm broad band probe and operating at 500.13 MHz (^1H), 125.77 MHz (^{13}C), 99.36 MHz (^{29}Si), and 202.45 MHz (^{31}P). The ^{29}Si NMR data were obtained using $^1H-^{29}Si$ HMQC experiments. Chemical shifts are reported in ppm downfield from internal $SiMe_4$ (^1H, ^{13}C, ^{29}Si), and external 85% H_3PO_4 (^{31}P); coupling constants are given in Hz. Bruker XWINNMR software was used for all processing.

X-ray Crystallography. General Considerations. The single-crystal analyses were carried out at the UC Berkeley CHEXRAY crystallographic facility. Measurements were made on a Bruker SMART CCD area detector with graphite-monochromated Mo Kα radiation ($\lambda = 0.710\,69$ Å). Data were integrated by the program SAINT, corrected for Lorentz and polarization effects, and analyzed for agreement and possible absorption using XPREP. Empirical absorption corrections were made using SADABS. Structures were solved by direct methods and expanded using Fourier techniques. The quantity minimized by the least-squares program was $\sum w(|F_o| - |F_c|)$,[70] where w is the weight of a given observation. The analytical forms of the scattering factor tables for the neutral atoms were used, and all scattering factors were corrected for both the real and the imaginary components of anomalous dispersion. All calculations were performed using the teXsan crystallographic software package. Selected crystal and structure refinement data are summarized in Tables 2 and 6. All crystals were mounted on a glass fiber using Paratone N hydrocarbon oil.

Considerations for 4a. Crystallization via slow diffusion of pentane into a toluene/THF solution of **4a** provided X-ray-quality crystals. The molecule packs in the unit cell with one moderately well-defined molecule of toluene and a poorly defined mass of electron density that might correspond to one tetrahydrofuran per two molecules of **4a**. This was assumed in determining the unit cell contents for the purposes of calculating F_{000} and the density. The model for the disordered solvent was five half-occupancy carbon atoms, since there was no way to assign one of them as a likely oxygen atom. All non-hydrogen atoms were refined anisotropically, except for boron and the carbon atoms of the solvent molecule. Hydrogen atom positions were calculated but not refined.

Considerations for 5. Crystals suitable for X-ray diffraction studies were grown over several days from a toluene solution that had been layered with ether. There are two unique molecules (which are structurally similar) in the asymmetric unit. The iridium, phosphorus, and silicon atoms were refined anisotropically. Methylene (CH_2) and methyl (CH_3) carbon atoms were refined anisotropically, while the phenyl (CH) carbon atoms were refined isotropically, and the hydrogen atom positions were calculated but not refined.

Considerations for 6. Crystals suitable for X-ray diffraction studies were grown over several days by the slow evaporation of a benzene solution of **6**. The iridium, phosphorus, and germanium atoms were refined anisotropically, the carbon and boron atoms were refined isotropically, and all hydrogen positions were calculated but not refined.

Considerations for 7b. Crystals suitable for X-ray diffraction studies were grown over several days by the slow cooling of a toluene/ether solution to −35 °C. The iridium, phosphorus, and silicon atoms were refined anisotropically, the carbon and boron atoms were refined isotropically, and all hydrogen positions were calculated but not refined.

Considerations for 8a. Crystals suitable for X-ray diffraction were grown over several days by the slow cooling of a toluene solution to −35 °C. The iridium, phosphorus, silicon,

---

[66] Mitchell, G. P.; Tilley, T. D. *Organometallics* **1998**, *17*, 2912.

[67] Braddock-Wilking, J.; Schieser, M.; Brammer, L.; Huhmann, J.; Shaltout, R. *J. Organomet. Chem.* **1995**, *499*, 89.

[68] Cooke, J. A.; Dixon, C. E.; Netherton, M. R.; Kollegger, G. M.; Baines, R. M. *Synth. React. Inorg. Met.-Org. Chem.* **1996**, *26*, 1205.

[69] Smit, C. N.; Bickelhaupt, F. *Organometallics* **1987**, *6*, 1156.

[70] SAINT: SAX Area-Detector Integration Program, version 4.024; Bruker Inc., Madison, WI, 1995.

and carbon atoms were refined anisotropically, with the exception of the carbon atoms of the disordered cyclooctyl ring. The cyclooctyl ring was modeled as 14 partial-occupancy carbon atoms. The positions and occupancies of these carbon atoms were refined, while the B_{iso} value for each atom was fixed at 9.5. The sum of the occupancies for these carbon atoms is 8. The boron atom was refined isotropically, and the hydrogen atom positions were calculated but not refined.

***fac*-$\mathbf{(Me_3P)_3Ir(SiHMes_2)(Me)(H)}$ (1).** A Schlenk tube containing a magnetic stir bar was charged with $\mathrm{(Me_3P)_4IrMe}$ (0.658 g, 1.29 mmol) and $\mathrm{H_2SiMes_2}$ (0.368 g, 1.37 mmol). Diethyl ether (20 mL) was added, and the resulting reaction solution was stirred rapidly. After 2−3 min **1** began to precipitate. The mixture was stirred for 7.5 h, filtered, and evaporated to dryness to give 0.558 g of analytically pure **1.** The filtrate was concentrated slightly and stored for 3 days at room temperature. An additional 0.104 g of crystalline **1** was then isolated by filtration (total yield 73%). ^{1}H NMR (benzene-d_6): δ 6.85 (s, 4 H, aryl), 5.93 (m, 1 H, SiH), 2.89 (br s, 12 H, ortho 2,4,6-$\mathit{Me}_3\mathrm{C_6H_2}$), 2.21 (s, 6 H, para 2,4,6-$\mathit{Me}_3\mathrm{C_6H_2}$), 1.14 (d, J_{HP} = 70 Hz, 9 H, PMe_3), 1.11 (d, J_{HP} = 76 Hz, 9 H, PMe_3), 1.06 (d, J_{HP} = 71 Hz, 9 H, PMe_3), 0.09 (m, 3 H, IrMe), −11.47 (dt, $^2J_{\mathrm{HP(trans)}}$ = 128 Hz, $^2J_{\mathrm{HP(cis)}}$ = 17 Hz, 1 H, IrH). ^{31}P{^{1}H} NMR (benzene-d_6): δ −63.3 (dd, $^2J_{\mathrm{PP}}$ = 19 Hz, $^2J_{\mathrm{PP}}$ = 14 Hz), −64.1 (dd, $^2J_{\mathrm{PP}}$ = 19 Hz, $^2J_{\mathrm{PP}}$ = 14 Hz), −64.7 (br). ^{29}Si{^{1}H} NMR (benzene-d_6): δ −46.7 (d, $^1J_{\mathrm{SiH}}$ = 151 Hz). ^{13}C{^{1}H} NMR (toluene-d_8): δ 144.1 (Si−C), 135.1 (aryl), 134.6 (2,4,6-$\mathrm{Me_3}\mathit{C}_6\mathrm{H_2}$), 129.1 (2,4,6-$\mathrm{Me_3}\mathit{C}_6\mathrm{H_2}$), 24.8 (2,4,6-$\mathit{Me}_3\mathrm{C_6H_2}$), 20.7 (2,4,6-$\mathit{Me}_3\mathrm{C_6H_2}$), 23.0 (dm, $^1J_{\mathrm{CP}}$ = 28 Hz, PMe_3), 21.2 (dm, $^1J_{\mathrm{CP}}$ = 27 Hz, PMe_3), 17.8 (dm, $^1J_{\mathrm{CP}}$ = 29 Hz, PMe_3). IR (Nujol, cm^{-1}): 2133 m (IrH), 2075 m (SiH). Anal. Calcd for $\mathrm{C_{28}H_{54}IrP_3Si}$: C, 47.77; H, 7.73. Found: C, 47.44; H, 7.53. Mp: 124−127 °C.

[*fac*-$\mathbf{(Me_3P)_3(H)_2Ir{=}SiMes_2][MeB(C_6F_5)_3]}$ (2). A $\mathrm{CH_2Cl_2}$ solution (10 mL) of $\mathrm{B(C_6F_5)_3}$ (0.314 g, 6.13 mmol) was added via cannula to **1** (0.428 g, 6.08 mmol) in $\mathrm{CH_2Cl_2}$ (10 mL) to give a yellow solution, which was stirred for 5 min. Removal of solvent under reduced pressure resulted in formation of a yellow powder which was analytically pure. Yield: 0.652 g (88%). ^{1}H NMR ($\mathrm{CD_2Cl_2}$): δ 6.85 (s, 4 H, 2,4,6-$\mathrm{Me_3C_6}\mathit{H}_2$), 2.53 (s, 12 H, ortho 2,4,6-$\mathit{Me}_3\mathrm{C_6H_2}$), 2.28 (s, 6 H, para 2,4,6-$\mathit{Me}_3\mathrm{C_6H_2}$), 1.78 (d, $^2J_{\mathrm{HP}}$ = 9 Hz, 9 H, PMe_3[trans to $\mathrm{SiMes_2}$]), 1.62 (d, $^2J_{\mathrm{HP}}$ = 8 Hz, 18 H, PMe_3), 0.52 (br, 3 H, B-Me), −11.02 (dm, $^2J_{\mathrm{HP(trans)}}$ = 84 Hz, 2 H, IrH). ^{31}P{^{1}H} NMR ($\mathrm{CD_2Cl_2}$): δ −63.0 (m), −63.8 (m), −64.4 (m). ^{29}Si{^{1}H} NMR ($\mathrm{CD_2Cl_2}$): δ 254.1 (d, $^2J_{\mathrm{SiP}}$ = 168 Hz). ^{13}C{^{1}H} NMR ($\mathrm{CD_2Cl_2}$): δ 149.9 (aryl), 148.0 (aryl), 135.8 (m, C−F), 145.3 (Si-C), 141.8 (aryl), 140.0 (aryl), 129.9 (Mes aryl), 24.88 (dm, $^1J_{\mathrm{CP}}$ = 30 Hz PMe_3), 24.5 (ortho 2,4,6-$\mathit{Me}_3\mathrm{C_6H_2}$), 23.7 (m, P$\mathit{Me}_3$), 21.3 (para 2,4,6-$\mathit{Me}_3\mathrm{C_6H_2}$). IR (Nujol, cm^{-1}): 2357 m (IrH). Anal. Calcd for $\mathrm{C_{46}H_{54}BF_{15}IrP_3Si}$: C, 45.44; H, 4.48. Found: C, 45.38; H, 4.29. Mp: 64−69 °C dec.

$\mathbf{[PhBP_3](H)_2Ir{=}SiMes_2}$ (4a). $\mathrm{[PhBP_3]Ir(\eta^3\text{-}C_8H_{13})(H)}$ (0.225 g, 0.228 mmol) was dissolved in benzene (5 mL). This solution was then transferred into a vessel containing dimesitylsilane, $\mathrm{H_2SiMes_2}$ (0.0611 g, 0.228 mmol). The resulting colorless, homogeneous solution was then warmed to 95 °C, and it gradually turned yellow within 4−5 h. After 24 h the volatile materials were removed under reduced pressure. Extraction with toluene (5 mL) and filtration removed a light yellow precipitate and afforded a deep yellow filtrate. This filtrate, which was dried in vacuo, contained yellow **4a** (0.221 g) as the only product identified by ^{1}H and ^{31}P{^{1}H} NMR spectroscopy. High-yield crystallization of this crude powder was difficult. However, analytically and spectroscopically pure material was precipitated via pentane addition to a toluene solution of **4a**, yielding 0.176 g (67%). A crystal suitable for an X-ray diffraction study was obtained by slow diffusion of pentane into a toluene/THF mixture (10:1) at 25 °C. ^{1}H NMR (benzene-d_6): δ 8.10−6.7 (m, 35 H, $\mathrm{PhBP_3}$ aryl), 6.63 (s, 2 H, 2,4,6-$\mathrm{Me_3C_6}\mathit{H}_2$), 2.50 (s, 12 H, ortho 2,4,6-$\mathit{Me}_3\mathrm{C_6H_2}$), 2.08 (s, 6 H, para 2,4,6-$\mathit{Me}_3\mathrm{C_6H_2}$), 1.93 (m, 4 H, $\mathrm{PhB(CH'_2PPh_2)(C}\mathit{H}_2\mathrm{PPh_2)_2}$), 1.83 (m, 2 H, $\mathrm{PhB(C}\mathit{H'}_2\mathrm{PPh_2)(CH_2PPh_2)_2}$), −9.47 (m, $^2J_{\mathrm{HP(trans)}}$ = 70 Hz, 2 H, IrH). ^{29}Si{^{1}H} NMR (benzene-d_6): δ 241.2 (dt, $^2J_{\mathrm{SiP(trans)}}$ = 172.4 Hz, $^2J_{\mathrm{SiP(cis)}}$ = 4 Hz). ^{31}P{^{1}H} NMR (benzene-d_6): δ 3.44 (t, J_{PP} = 18 Hz), 2.24 (d, J_{PP} = 18 Hz). ^{13}C{^{1}H} NMR (THF-d_8): δ 140.5 (aryl), 139.7 (aryl), 133.2 (aryl), 133.1 (aryl), 132.6 (aryl), 132.4 (aryl), 129.8 (aryl), 129.2 (aryl), 129.1 (aryl), 128.9 (aryl), 124.5 (aryl), 24.5 (ortho 2,4,6-$\mathrm{Me_3C_6H_2}$), 21.4 (para 2,4,6-$\mathrm{Me_3C_6H_2}$), 18.0 (br, $\mathrm{BCH_2P}$). IR (Nujol, cm^{-1}): 3055 m, 2958 m, 2923 m, 2122 m, 2060 m (IrH), 1064 w, 1482 m, 1417 s, 1262 w, 1159 m, 1096 s, 1027 m, 924 m, 862 w, 803 w, 740 m, 697 s, 517 m. Anal. Calcd for $\mathrm{C_{63}H_{65}BIrP_3Si}$: C, 66.01; H, 5.72. Found: C, 65.76; H, 5.90.

Observations of $\mathbf{[PhBP_3](H)_2Ir{=}SiR_2}$. For R = Ph (4b). An NMR tube containing a benzene-d_6 solution of **3** (0.024 g, 0.024 mmol) and $\mathrm{Ph_2SiH_2}$ (0.005 g, 0.03 mmol) was heated at 80 °C for 24 h. Analysis of the reaction mixture by ^{1}H, ^{31}P{^{1}H), and ^{29}Si{^{1}H} NMR spectroscopy revealed nearly complete conversion (ca. 85%) to $\mathrm{[PhBP_3](H)_2Ir{=}SiPh_2}$ and COE. ^{1}H NMR (benzene-d_6): δ 8.11, 7.98, 7.76, 7.66, 7.41, 7.05, 6.67, 6.65 (aryl), 1.97 (m, 4 H, $\mathrm{PhB(CH'_2PPh_2)(C}\mathit{H}_2\mathrm{PPh_2)_2}$), 1.85 (m, 2 H, $\mathrm{PhB(C}\mathit{H'}_2\mathrm{PPh_2)(CH_2PPh_2)_2}$), −9.46 (dm, $^2J_{\mathrm{HP(trans)}}$ = 75 Hz, 2 H, IrH). ^{31}P{^{1}H} NMR (benzene-d_6): δ 5.41 (d, $^2J_{\mathrm{PP}}$ = 19 Hz, 2 P, trans to H), 3.50 (t, $^2J_{\mathrm{PP}}$ = 19 Hz, 1 P, trans to Si). ^{29}Si{^{1}H} (benzene-d_6): δ 327.5.

For R = Et (4c). An NMR tube containing a benzene-d_6 solution of **3** (0.017 g, 0.017 mmol) and $\mathrm{Et_2SiH_2}$ (0.005 g, 0.05 mmol) was allowed to sit at room temperature for 12 h. Analysis by ^{1}H, ^{31}P{^{1}H}, and ^{29}Si{^{1}H}NMR spectroscopy revealed nearly complete conversion to $\mathrm{[PhBP_3](H)_2Ir{=}SiEt_2}$ and COE. ^{1}H NMR (benzene-d_6): δ 8.13, 7.78, 7.68, 7.57, 7.43, 7.12, 7.00, 6.81 (aryl), 1.92 (m, 4 H, $\mathrm{PhB(CH'_2PPh_2)(C}\mathit{H}_2\mathrm{PPh_2)_2}$), 1.80 (m, 2 H, $\mathrm{PhB(C}\mathit{H'}_2\mathrm{PPh_2)(CH_2PPh_2)_2}$), −10.13 (dm, $^2J_{\mathrm{HP(trans)}}$ = 76 Hz, 2 H, IrH). ^{31}P{^{1}H} NMR (benzene-d_6): δ 6.23 (d, $^2J_{\mathrm{PP}}$ = 19 Hz, 2 P, trans to H), 2.21 (t, $^2J_{\mathrm{PP}}$ = 19 Hz, 1 P, trans to Si). ^{29}Si{^{1}H}(benzene-d_6): δ 307.4.

For R = Me (4d). A PTFE-capped NMR tube containing a benzene-d_6 solution of **3** (0.018 g, 0.018 mmol) was degassed by two freeze−pump−thaw cycles, and an atmosphere of $\mathrm{Me_2SiH_2}$ was introduced. The tube was then sealed, and the solution was heated at 80 °C for 2 min. Analysis by ^{1}H, ^{31}P{^{1}H}, and ^{29}Si{^{1}H} NMR spectroscopy revealed nearly complete conversion (ca. 90%) to $\mathrm{[PhBP_3](H)_2Ir{=}SiMe_2}$ and COE. ^{1}H NMR (benzene-d_6): δ 7.71−6.76 (35 H, aryl), 0.35 (s, 9 H, SiMe_3), −10.17 (dm, $^2J_{\mathrm{HP(trans)}}$ = 69 Hz, 2 H, IrH). ^{31}P{^{1}H} NMR (benzene-d_6): δ 4.76 (d, $^2J_{\mathrm{PP}}$ = 20 Hz, 2 P, trans to H), 2.59 (t, $^2J_{\mathrm{PP}}$ = 20 Hz, 1 P, trans to Si). ^{29}Si{^{1}H}(benzene-d_6): δ 311.2.

$\mathbf{[PhBP_3](H)_2Ir{=}GeMes_2}$ (6). In a PTFE-sealed reaction vessel, a 4 mL benzene solution of $\mathrm{[PhBP_3]Ir(\eta^3\text{-}C_8H_{13})H}$ (0.102 g, 0.103 mmol) and $\mathrm{Mes_2GeH_2}$ (0.031 g, 0.099 mmol) was stirred at 83 °C for 36 h. The solvent was removed in vacuo to give a yellow oil, which was triturated with 4 mL of benzene to yield an orange powder. The powder was crystallized by layering a 2 mL toluene solution with 3 mL of $\mathrm{Et_2O}$ and storing at −35 °C; from this, yellow crystals were obtained (0.084 g, 76%). ^{1}H NMR (benzene-d_6): δ 8.01−6.73 (35 H, $\mathrm{[PhBP_3]}$ aryl), 6.66 (s, 4 H, ortho 2,4,6-$\mathrm{Me_3C_6}\mathit{H}_2$), 2.54 (s, 12 H, ortho 2,4,6-$\mathit{Me}_3\mathrm{C_6H_2}$), 2.15 (s, 6 H, para 2,4,6-$\mathit{Me}_3\mathrm{C_6H_2}$), 1.89 (br, 2 H $\mathrm{B(CH_2P)_2(C}\mathit{H'}_2\mathrm{P')}$), 1.82 (br, 2 H $\mathrm{B(C}\mathit{H}_2\mathrm{P)_2(CH'_2P')}$), −9.68 (dm, $^2J_{\mathrm{HP}}$ = 83 Hz, 2 H, IrH). ^{31}P{^{1}H} NMR (benzene-d_6): δ 6.12 (t, $^2J_{\mathrm{PP}}$ = 19 Hz, 2 P, trans to H), 3.61 (d, $^2J_{\mathrm{PP}}$ = 19 Hz, 1 P, trans to Ge). ^{13}C{^{1}H} NMR (benzene-d_6): δ 138.8 (aryl), 133.2 (aryl), 132.3 (aryl), 131.9 (aryl), 129.8 (aryl), 129.7 (aryl), 128.5 (aryl), 127.3 (aryl), 125.6 (aryl), 124.2 (aryl), 23.1 (ortho 2,4,6-$\mathit{Me}_3\mathrm{C_6H_2}$), 21.0 (para 2,4,6-$\mathit{Me}_3\mathrm{C_6H_2}$), 17.6 (br, $\mathrm{B}\mathit{C}\mathrm{H_2P}$). IR (KBr, cm^{-1}): 3052 m, 2917 m, 2061 br m (IrH), 1618 m, 1434 s, 1330 s, 1090 s, 924 m, 812 s, 697 s. Anal. Calcd for $\mathrm{C_{63}H_{65}BIrP_3Ge}$: C, 63.55; H, 5.50. Found: C, 63.83; H, 5.67. Mp: 134−137 °C dec.

$\mathbf{[PhBP_3]IrH_3(SiEt_3)}$ (7a). In a PTFE-sealed reaction vessel, $\mathrm{[PhBP_3]Ir(\eta^3\text{-}C_8H_{13})H}$ (0.091 g, 0.092 mmol) and $\mathrm{Et_3SiH}$ (0.011

g, 0.092 mmol) were combined with 4 mL of benzene. The reaction mixture was stirred and heated at 50 °C for 2 days. Removal of the volatile materials yielded an oily solid, which was triturated with 4 mL of pentane to give a yellow solid (0.035 g, 38%). ^{1}H NMR (benzene-d_6): δ 8.23−6.84 (35 H, [PhBP$_3$] aryl), 1.93 (br, 6 H, BCH_2P), 1.37 (q, J = 8 Hz, 6 H, SiCH_2CH$_3$), 1.08 (t, J = 8 Hz, 9 H, SiCH$_2$CH_3), −11.0 (dm, $^2J_{\mathrm{HP(trans)}}$ = 64 Hz, 3 H, IrH). ^{31}P{^{1}H} NMR (benzene-d_6): δ −5.52 (s). ^{13}C{^{1}H} NMR (benzene-d_6): δ 140.1 (aryl), 133.3 (aryl), 132.7 (aryl), 129.4 (aryl), 129.1 (aryl), 128.3 (aryl), 124.9 (aryl), 17.5 (q, $^3J_{\mathrm{CP}}$ = 2 Hz, SiCH$_2$CH$_3$), 16.5 (br, BCH$_2$P), 9.2 (SiCH$_2$$CH_3$). IR (KBr, cm^{-1}): 3056 m, 2904 m, 2871 m, 2081 br m (IrH), 1482 m, 1434 s, 1159 w, 1091 s, 1002 w, 923 m, 891 w, 861 w, 738 s, 694 w, 516 s, 480 m. Anal. Calcd for $C_{51}H_{59}SiBP_3$: C, 61.50; H, 5.97. Found: C, 61.78; H, 6.00. Mp: 207−216 °C dec, 216−219 °C (melt).

[PhBP$_3$]IrH$_3$(SiMe$_3$) (7b). In a PTFE-sealed reaction vessel, a 4 mL benzene solution of [PhBP$_3$]Ir(η^3-C$_8$H$_{13}$)H (0.212 g, 0.214 mmol) was degassed by three freeze−pump−thaw cycles, and an atmosphere of Me$_3$SiH was introduced. The vessel was then placed in an oil bath maintained at 75 °C for 6 days, after which time the solvent was removed in vacuo. The resulting oil was washed with pentane (3 × 5 mL) to give a tan powder (0.135 g, 66%). ^{1}H NMR (benzene-d_6): δ 8.13 (d, J = 7 Hz, 2 H, aryl), 7.68 (t, J = 7 Hz, 2 H, aryl), 7.46 (m, 13 H, aryl), 6.78 (m, 18 H, aryl), 1.83 (m, 6 H, BCH_2P), 1.06 (s, 9 H, SiMe_3), −10.6 (dm, $^2J_{\mathrm{HP(trans)}}$ = 81 Hz, 3 H, IrH). ^{31}P{^{1}H} NMR (benzene-d_6): δ −3.81. ^{29}Si{^{1}H} NMR (benzene-d_6): δ −21.4. ^{13}C{^{1}H} NMR (benzene-d_6): δ 140.1 (d, J = 50 Hz, aryl), 132.8 (s, aryl), 132.6 (m, aryl), 129.3 (s, aryl), 128.2 (m, aryl), 16.6 (br, BCH$_2$P), 16.4 (q, $^3J_{\mathrm{CP}}$ = 3 Hz). IR (KBr, cm^{-1}): 3055 m, 2941 w, 2889 w, 2091 br m (IrH), 1483 m, 1433 s, 1259 m, 1159 m, 1092 s, 922 s, 827 s, 739 s, 694 s, 628 m. Anal. Calcd for $C_{48}H_{53}BSiIrP_3$: C, 60.43; H, 5.60. Found: C, 60.11; H, 5.57. Mp: 191−197 °C dec, 213−220 °C (melt).

[PhBP$_3$](H)$_2$Ir=Si(Mes)(C$_8$H$_{15}$) (8a). A 1 mL benzene solution of MesSiH$_3$ was added to a 5 mL benzene solution of **3**, and the reaction mixture was stirred at room temperature for 24 h. The solvent was removed under reduced pressure to give a yellow oil. This was dissolved in 1 mL of THF, and slow diffusion of Et$_2$O at −35 °C yielded tan crystals of **8a** (0.158 g, 75%). ^{1}H NMR (benzene-d_6): δ 8.80−6.52 (35 H, aryl), 2.43 (br, 6 H, BCH_2P), 2.19 (s, 6 H, ortho 2,4,6-Me_3C$_6$H$_2$), 2.03 (s, 3 H, para 2,4,6-Me_3C$_6$H$_2$), 2.03−1.76 (m, 15 H, cyclooctyl), −10.00 (dm, $^2J_{\mathrm{HP(trans)}}$ = 76 Hz, 2 H, IrH). ^{31}P{^{1}H} NMR (benzene-d_6): δ 2.20 (t, $^2J_{\mathrm{PP}}$ = 19 Hz, 1 P, trans to Si), 1.41 (d, $^2J_{\mathrm{PP}}$ = 19 Hz, 2 P, trans to H). ^{29}Si{^{1}H} NMR (benzene-d_6): δ 274.2 (d, $^2J_{\mathrm{SiP(trans)}}$ = 158 Hz). ^{13}C{^{1}H} NMR (benzene-d_6): 145.7 (aryl), 141.4 (aryl), 140.5 (aryl), 139.1 (aryl), 139.0 (aryl), 133.1 (aryl), 132.8 (aryl), 132.5 (aryl), 129.5 (aryl), 129.1 (aryl), 127.8 (aryl), 124.7 (aryl), 45.9 (d, $^3J_{\mathrm{CP}}$ = 7 Hz, SiCH assigned using a DEPT 90 experiment), 30.0 (cyclooctyl CH$_2$), 28.3 (cyclooctyl CH$_2$), 27.8 (cyclooctyl CH$_2$), 25.9 (cyclooctyl CH$_2$), 22.8 (ortho 2,4,6-Me_3C$_6$H$_2$), 21.5 (para 2,4,6-Me_3C$_6$H$_2$), 17.1 (br, BCH$_2$P). IR (KBr, cm^{-1}): 3055 m, 2917 s, 2851 m, 2090 m (IrH), 1482 m, 1433 s, 1159 w, 1091 s, 921 m, 890 w, 864 w, 790 w, 749 s, 738 s, 696 s, 518 s, 478 w, 421 w. Anal. Calcd for $C_{62}H_{69}SiBIrP_3$: C, 65.42; H, 6.11. Found: C, 65.15; H, 6.31. Mp: 240−244 °C dec.

[PhBP$_3$](H)$_2$Ir=Si(Trip)(C$_8$H$_{15}$) (8b). A 4 mL toluene solution containing **3** (0.170 g, 0.172 mmol) and TripSiH$_3$ (0.040 g, 0.171 mmol) was stirred for 3 days. The reaction mixture was concentrated under reduced pressure to ca. 1.5 mL. The slow diffusion of pentane into the resulting toluene solution (room temperature) afforded yellow, crystalline **8b** (0.097 g, 47%), which was isolated by filtration and washed with pentane (2 × 1 mL). ^{1}H NMR (benzene-d_6): δ 8.18−6.68 (37 H, aryl), 3.67 (sept, J = 6 Hz, 2 H, ortho CHMe$_2$), 2.97 (sept, J = 6 Hz, 1 H, para CHMe$_2$), 2.38 (br, 6 H, BCH_2P), 2.03−1.76 (m, 15 H, cyclooctyl), 1.27 (d, J = 6 Hz, 12 H, ortho CHMe_2), 1.19 (d, J = 6 Hz, 6 H, para CHMe_2), −10.12 (dm, $^2J_{\mathrm{HP}}$ = 71 Hz, 2 H, IrH). ^{31}P{^{1}H} NMR (benzene-d_6): δ 2.80 (t, $^2J_{\mathrm{PP}}$ = 18 Hz, 1 P, trans to Si), 1.77 (d, $^2J_{\mathrm{PP}}$ = 18 Hz, 2 P, trans to H). ^{29}Si{^{1}H} NMR (benzene-d_6): δ 317.1. ^{13}C{^{1}H} NMR (benzene-d_6): 151.4, 150.8, 141.7, 133.6, 132.7, 129.7, 126.0, 124.8, 124.6, 122.1, 121.8 (aryl), 39.2 (SiCH), 31.1 (cyclooctyl CH$_2$), 29.8 (cyclooctyl CH$_2$), 28.9 (cyclooctyl CH$_2$), 26.9 (cyclooctyl CH$_2$), 22.9 (Trip Me), 21.8 (Trip Me), 18.3 (br, BCH$_2$P). IR (KBr, cm^{-1}): 3056 m, 2955 m, 2918 m, 2137 br m (IrH), 1482 m, 1434 s, 1159 w, 1089 s, 925 m, 863 w, 739 s, 695 s, 519 s, 482 m. Anal. Calcd for $C_{68}H_{81}SiBIrSiP_3$: C, 66.81; H, 6.68. Found: C, 66.95; H, 6.30. Mp: 189−193 dec.

Acknowledgment is made to the National Science Foundation for their generous support of this work. We than Dr. Fred Hollander of the UC Berkeley CHEXRAY facility for assistance with the X-ray structure determinations and for solving the structures for **4a** and **8b**.

Supporting Information Available: Tables of crystal, data collection, and refinement parameters, bond distances and angles, and anisotropic displacement parameters for **4a**, **5**, **6**, **7b**, and **8b**. This material is available free of charge via the Internet at http://pubs.acs.org.

OM020389U